Numerical Simulation of the Flow in the Large Aspect Ratio Pipe with the Viscoelasticity Effect of Blood Vessel Wall

Aya SAITO and Tetuya KAWAMURA

(Received July 3, 2014)

Abstract

Kawasaki Disease was first found by M.D. Kawasaki in 1961 and reported in 1967. Children under four years tend to suffer from this disease. It is a kind of vasculitis syndrome and some patients may have aneurysms in the coronary arteries of the heart or others may have the risk of atheorosclerosis after the condition of patients getting better. The cause of this disease has not been revealed so far and the internal flow field in the vessel has not been disclosed yet. Most of studies about the flow in the coronary arteries treat the vessel wall as non-viscoelastic one. However, the real vessel wall has viscoelasticity and it may affect both vessel deformation and the flow fields in the blood vessel. In this research, the simulation in long pipe having viscoelasticity is accomplished as the first step of numerical analysis in a coronary artery. In the results, it is observed that the difference exists between the flow fields in the pipe with and without viscoelasticity.

1. Introduction

Recently, the number of patients of Kawasaki Disease has increased (Year 1996 : 100 patients →Year 2006 : 190 patients / 0~4 year old 100,000 children)[1]. The symptoms of this disease are the dropsy that appears on hands or feet, a high fever lasting for more than five days, and so on. These symptoms are developed by the vasculitis. However, the cause of this disease has not been revealed yet. A cure method has been established these days to some extent although there is small possibility that large aneurysms is left in the coronary arteries after the recovery. These aneurysms can be stitched and reduced by surgery. But the precise index indicating the reduction of the aneurysms that permit the blood flow without bad effect on the blood flow has not been known. Other patients escaping from the aneurysms may have the risk of atherosclerosis for years because the inner wall of the blood vessel experiences inflammation and is injured before the recovery. However, since Kawasaki Disease was announced officially in 1967 first in the world, the influence long after the recovery has not been identified.

The damaged part is in the heart so that it is difficult to investigate. Moreover, the region affected by the disease is smaller than other vasculitis syndrome because the most of patients are children. Due to these difficulties, the internal phenomenon of blood vessel is hard to make clear. Therefore, the simulation is effective method to understand the flow in a coronary artery. The research concerning to the simulation of Kawasaki Disease is not only few, but also inaccurate because the vessel wall is assumed to be rigid [2]. However, it is not clear whether the assumption of viscoelasticity is necessary to investigate into a coronary artery or not. In this research, the flow in the long pipe with viscoelasticity is analyzed numerically to decide the necessity of assumption such that the blood vessel wall should have viscoelasticity as a first step of the flow simulation of a coronary artery affected by Kawasaki Disease.

2. Governing equations

Flows in a straight pipe, and in a combination of a straight pipe and a 90 degree bended pipe as shown in Fig.1 and Fig.2 are computed. The aspect ratio (pipe length / initial pipe diameter) is 25 in two cases. The oscillating flow is coming into the pipe. The fluid is incompressible and Newtonian [3]. This flow is governed by equation of continuity (Eq. (1)) and Navier-Stokes equation that is non-dimensionalized by physical quantity of the oscillatory flow (Eq. (2)),

$$\nabla \cdot \boldsymbol{v} = 0 \qquad (1)$$

$$\frac{Wo^2}{Re}\frac{\partial \boldsymbol{v}}{\partial t} + (\boldsymbol{v}\cdot\nabla)\boldsymbol{v} = -\,\mathrm{grad}\, p + \frac{1}{Re}(\Delta \boldsymbol{v}) \qquad (2)$$

where $Wo = L\sqrt{f/\nu}$ (f[Hz]: frequency of oscillatory flow, L[m]: characteristic length, ν[m^2/s]: kinematic viscosity) : Womersley Number, $Re = UL/\nu$ (U[m/s]: characteristic velocity), p[Pa]: pressure, t[s]: time, v: velocity of fluid. In the calculation with viscoelasticity, the diameter of the pipe is assumed to vary according to the force due to the fluid flow. Voigt Model in which a spring and a dashpot (Eq. (3)) are arranged in parallel is adopted as the model of viscoelasticity of the vessel wall. The variation of the pipe diameter is calculated by using the wall pressure that can be estimated by the blood vessel viscoelasticity that was measured experimentally [4]. The model of the vessel wall with viscoelasticity is,

$$p_{wall} = c \cdot \frac{\partial D(t)}{\partial t} + k \cdot D(t) \qquad (3)$$

where c[Pa・s]: viscosity of the vessel wall, D[m]: variation of the pipe diameter, k[Pa/%]: elasticity of the vessel wall, p_{wall}[Pa]: wall pressure. Moreover, as the diameter of the pipe is changed according to the pressure of the fluid at each time step, the general coordinate transformation is introduced into Eq. (2) so that it is possible to fit to temporal variation of the pipe diameter.

At first, the flow in the pipe (cross section: x, y plane, longitudinal direction: z axis) indicated in Fig.1 is calculated. Next, the flow in the 90 degree bended pipe shown in Fig.2 that is one model of a coronary artery is calculated.

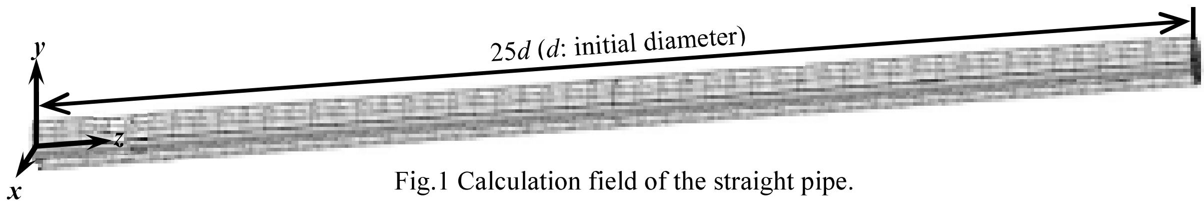

Fig.1 Calculation field of the straight pipe.

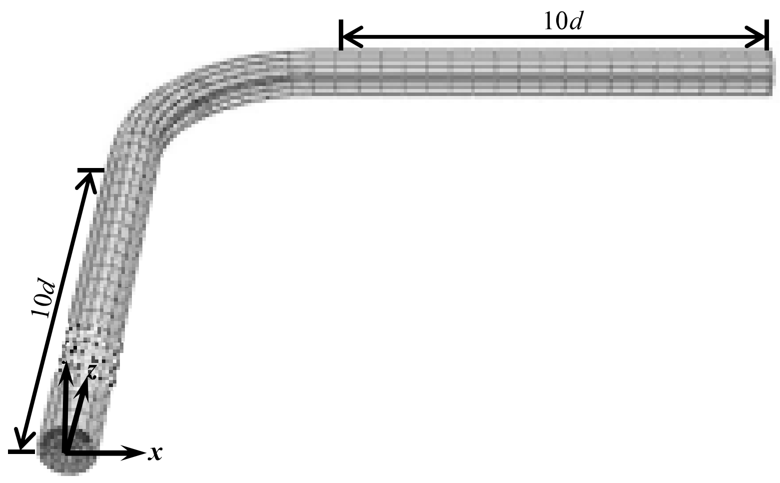

Fig.2 Calculation field of 90 degree bended

3. Condition of calculation

At the inlet, two kinds of oscillatory flows, i.e. the simple sine wave and the flow pattern shown in Fig.3 that resembles the real flow in a coronary artery are given. At the outlet, the free outflow condition is adopted. Along the pipe wall, no-slip condition is imposed. Along the center line where the equation becomes singular, Neumann condition is applied. In the direction of pipe circumference, the periodic boundary condition is introduced. Three dimensional calculation is performed. Time interval, DT, is 1.0×10^{-4}. The flow is calculated during five oscillatory periods and the fifth period is investigated. The number of grid is, x direction : 21, y direction : 32, z direction : 501.

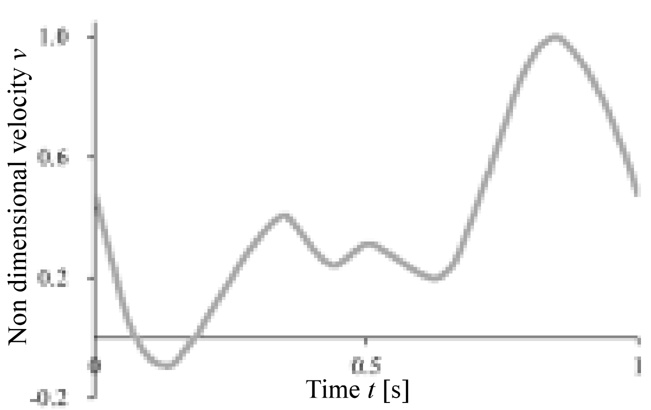

Fig. 3 Time history of velocity pattern at the inlet of the coronary

Fractional step method is employed in this study. In this method, first, provisional velocity is calculated at a certain time by quasi-Navier-Stokes equation in which pressure terms are omitted from original equaiton, next, such velocity is substituted into Poisson equation to calculate pressure, and finally, velocity at the next time is obtained from provisional velocity and pressure.

Physical parameters of the fluid and vessel wall are $\nu=3.3\times10^{-6}$[m^2/s], $c = 2.7\times10^3$[Pa· s], $k = 6.7\times10^2$[Pa/%].

4. Computational Result

4-1. In the straight pipe with the simple sine wave inflow

Firstly, the case of the simple sine wave flow coming into the straight pipe (Fig.1) is calculated. The flow condition is Re = 500 and Wo = 10, that is similar to the real blood flow in a coronary artery. The variation of the pipe diameter and shear stress with viscoelasticity is investigated and compared to the case without viscoelasticity.

The temporal variation rate of the pipe diameter during one period with and without viscoelasticity is shown in Fig.4. The symbols of circles, squares, and triangles in the figure represent the location of the flow, i.e. at the inlet of the pipe, at the middle in the longitudinal direction and at the outlet, respectively. The difference of the pipe diameter between the flow with and without viscoelasticity is the largest at the inlet, tend to become smaller downstream and hardly appear at the outlet. At the inlet and longitudinal middle, the pipe diameter is enlarged by the inflow during the time of 0 – 0.5s (the former half of the oscillation period) in the case with viscoelasticity. During the time of 0.5 – 1.0s (the latter half), the pipe diameter is reduced with decreasing of inflow velocity. From this result, the pipe diameter varies ± 1% in the case with viscoelasticity.

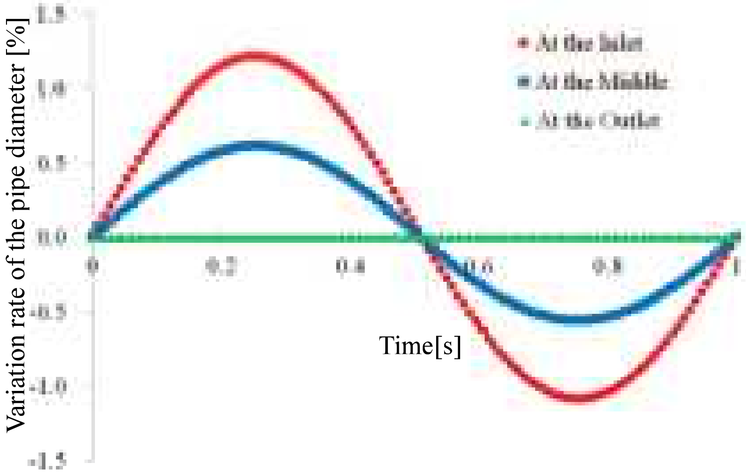

Fig.4 Comparison of temporal variation rate of the pipe diameter among three positions.

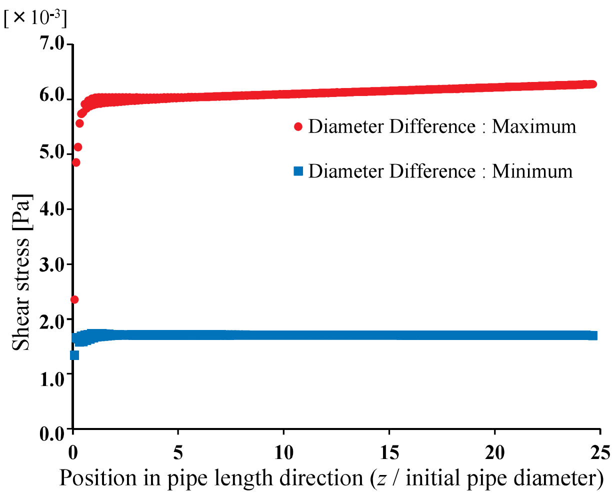

Fig.5 Shear stress in *z* direction at the different time.

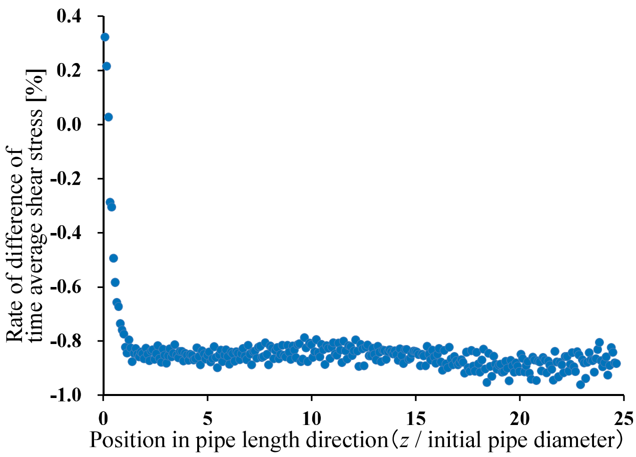

Fig.6 Difference of time average shear stress in *z* direction between with and without viscoelasticity.

Fig.5 shows the distribution of shear stress in the *z* direction in the case with viscoelasticity. The shear stress becomes three times larger at the time when the pipe diameter becomes the maximum in the period (t =0.25s in Fig.4) than at the time when it becomes the minimum (t =0.5s). Moreover, at t =0.25s, the shear stress increases slightly along *z* direction. The difference of time average shear stress in *z* direction between with and without viscoelasticity is shown in Fig.6. It is found that there is the difference about 1 % along almost all length of the pipe except for the region near the inlet.

4-2. In the 90 degree bended pipe with the real inflow wave of a coronary artery

Next, the flow is assumed to have the real inflow of a coronary artery flowing into the 90 degree bended pipe. The condition is Re =500 and Wo = 10, which is the same as the flow of the straight pipe.

The velocity vectors of the mainstream at t = 0.1 and 0.9s are shown in Fig.7-(a), and (b), respectively. At t = 0.1s, the direction of the flow is that from the outlet to the inlet (opposite direction). The adverse flow occurs also in the bended part. This indicates that the velocity in the outside of the bended part is kept to be positive even when the direction of inflow becomes opposite. This is because the outside velocity is larger than inside while the flow direction is positive and

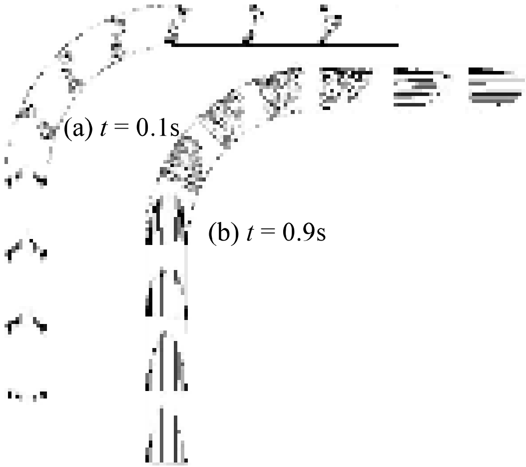

Fig.7 Velocity vectors in the 90 degree bended pipe.

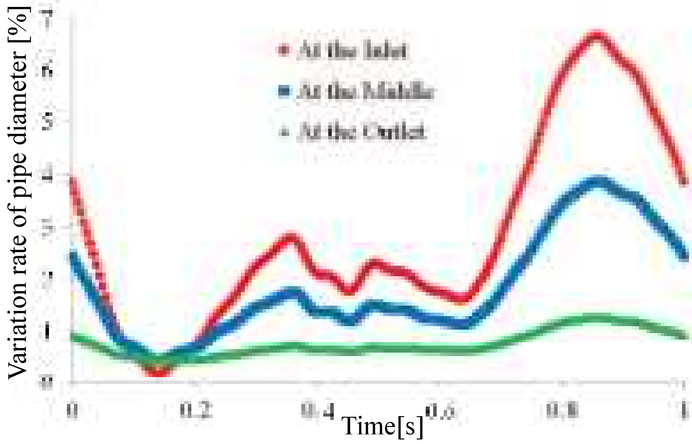

Fig.8 Comparison of temporal variation rate of 90 degree bended pipe diameter among three positions.

the relation is kept even when the direction of the inflow becomes opposite. At t = 0.9s when the inflow velocity becomes maximum, the velocity profile becomes asymmetric in the bended part and its downstream and the velocity in the outside is larger than in the inside.

Fig.8 shows the temporal variation rate of the pipe diameter in the case with and without viscoelasticity. The symbols of circles, squares, and triangles represent the location of the flow, i.e. at the inlet of the pipe, at the middle in the longitudinal direction and at the outlet, respectively, as in Fig.4. The variation of the pipe diameter corresponds to the tendency of the inflow. The diameter varies 7% at the vicinity of the inlet and 4% at the longitudinal middle.

Locations	Velocity Vectors	Pressure	Absolute value of mainstream velocity
Point **A** : The middle of bended part (z = 12.5d) 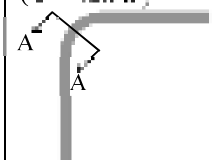	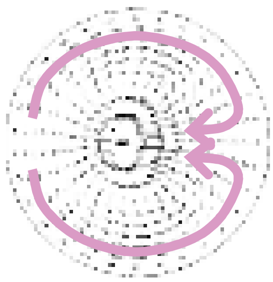	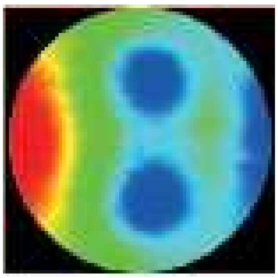	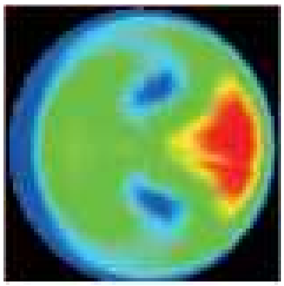
Point **B** : 5d from the inlet (z = 5d) 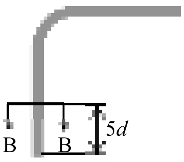		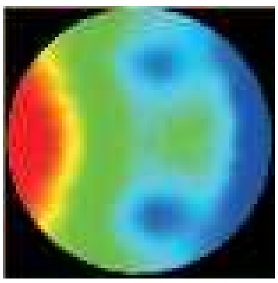	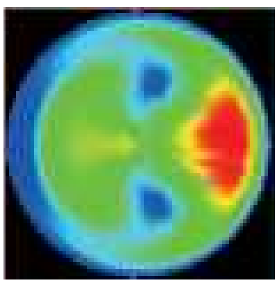

Fig.9-(a) Velocity vectors and pressure distributions in the cross sectional area (t = 0.1s)

Locations	Velocity Vectors	Pressure	Absolute value of mainstream velocity
Point **A** : The middle of bended part ($z = 12.5d$) 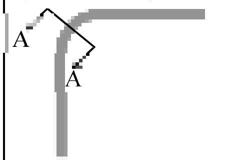			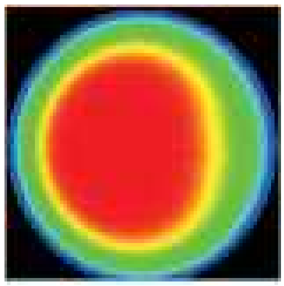
Point **B** : 5d from the inlet ($z = 5d$) 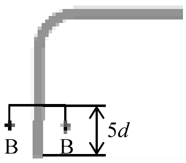	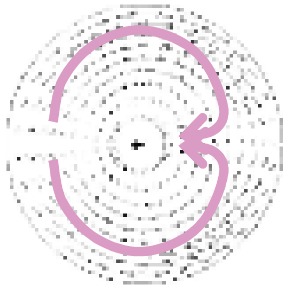		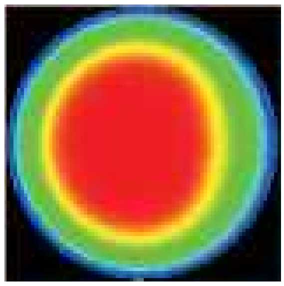

Fig.9-(b) Velocity vectors and pressure distributions in the cross sectional area (t = 0.9s)

Fig.9 shows the distribution of velocity vectors, pressure, and the magnitude of mainstream velocity in the cross sectional area. The upper panels show the results at the middle of the bended part (Point A in Fig.9) and the lower panels show those at the point in the straight part apart from the inlet by 5d (d : initial diameter)(Point B). Time is the same as Fig.7. At t = 0.1s (Fig.9-(a)), the secondary flow appears in the region from the outside of the bended part toward the inside at both points, A and B. At t = 0.1s, there are two regions of lower pressure as shown in Fig.9-(a) and at the same time, the adverse flow occurs (Fig.7-(a)) and the magnitude of the inside velocity is larger than the outside. At t = 0.9s (Fig.9-(b)), the secondary flow is strengthened in the bended part. Moreover, high pressure region in the outside of bended pipe and lower pressure region in the inside are extended respectively. The position of maximum flow velocity downstream of the bended part locates near the outer wall as shown in Fig.7-(b).

5. Conclusion

The flow in the straight pipe having the simple sine wave at the inlet and the flow in the 90 degree bended pipe having the real wave of a coronary artery at the inlet are calculated and the internal flow fields are investigated.

From examining the results in the both cases, it is observed that the variation of the pipe diameter and the magnitude of shear stress are influenced by viscoelasticity just a few percent. The typical syndrome of blood vessel that the patients of Kawasaki Disease may have in the future is atherosclerosis and this syndrome tends to occur at the region of lower wall shear stress [5]. The influence of viscoelasticity may correspond to this lower stress region. Therefore, the viscoelasticity should be taken into account with the calculation of the flow in a coronary artery because it is observed that, although it is small, there is a difference between with and without viscoelasticity cases.

References

[1] Ishii, M. and Igarashi, T., “All about Kawasaki Disease”, Nakayama Shoten, (2012)

[2] Sengupta, S. et al., “Image-based modeling of hemodynamics in coronary artery aneurysms caused by Kawasaki disease”, Biomech Model Mechanobiol, 11 (2012), pp. 915-932.

[3] Johnston, B. M., “Non-Newtonian blood flow in human right coronary arteries: Transient simulations”, Journal of Biomechanics, 39 (2006), pp. 1116-1128.

[4] Kohno, A. et al, “Quantitative Evaluation of Pain with Mechanical Nociceptive Stimuli by the Change of Arterial Wall Viscoelasticity”, The Japanese journal of medical instrumentation, 80 (2010), pp196-204

[5] Friedman, M. H., “Correlation between intimal thickness and fluid shear in human arteries”, 39 (1981), pp. 425-436.

Aya Saito
Graduate School of Humanities and Sciences, Advanced Sciences, Ochanomizu University
Otsuka 2-1-1, Bunkyo-ku, Tokyo 112-8610, Japan
E-mail: g1370610@edu.cc.ocha.ac.jp

Tetuya Kawamura
Graduate School of Humanities and Sciences, Ochanomizu University
E-mail : kawamura@is.ocha.ac.jp